Some similarities and differences in collisional electron loss of H^-, H_2^+, and He^+

M. M. Duncan and M. G. Menendez
Department of Physics and Astronomy, University of Georgia, Athens, Georgia 30602
(Received 22 September 1980)

We have measured the electron-loss peak as a function of angle for the following collisions at 0.5 MeV/amu: H_2^+-Ar, H_2^+-Ne, H_2^+-Kr, He^+-Kr, and H^--Kr. Electron energy spectra at an angle of 6° and complete angular distributions are shown for the last three systems listed above. The energy at which the electron-loss peak has its maximum and the width at half-maximum of the peak are compared for all five systems in the angular range $1.5 \leq \theta \leq 10°$. Our results suggest that, as previously indicated, the angular distribution of the electron-loss peak seems to be determined by the target. When the projectile is a positive ion the energy of the electron-loss peak seems to be independent of target or projectile and therefore is a general feature of the process. The width of the electron-loss peak and its dependence on angle seems to depend primarily on the projectile. Electron-scattering-model calculations do no predict features of the electron-loss peaks which are angular dependent.

I. INTRODUCTION

The collisional electron loss of fast projectiles, 0.5 MeV/amu, has been the subject of investigation at our laboratory for several years. The experiments use a cross-beam gas target and a hemispherical electron energy analyzer which can be positioned at any angle from 0° to 173° relative to the projectile beam. Electron energy spectra are measured at selected angles. These spectra show a prominent peak whose energy is centered near $E_e = \frac{1}{2} m_e v_i^2$, where v_i is the projectile velocity. As will be discussed below, for projectiles of interest here, the electrons in the peaks come primarily from the projectiles. Further details of the experimental arrangement and data reduction can be found in previous papers.[1,2] Examples of electron-loss peaks, corrected for the analyzer resolution and with background subtracted, can be seen in Fig. 1.

In recent papers on the electron loss of H^- and H in collisions with Ar and He, two characteristics of the results were noted.[1,2] First, the angular distributions obtained by integrating the counts under the electron-loss peak for each detection angle seemed similar in shape to the single differential cross sections (SDCS) obtained from the elastic scattering of electrons (moving with the same velocity as the H^- ion) by the target gas. Since H^- is such a weakly bound ion for single-electron loss such a result seemed reasonable, especially in the light of an electron-scattering

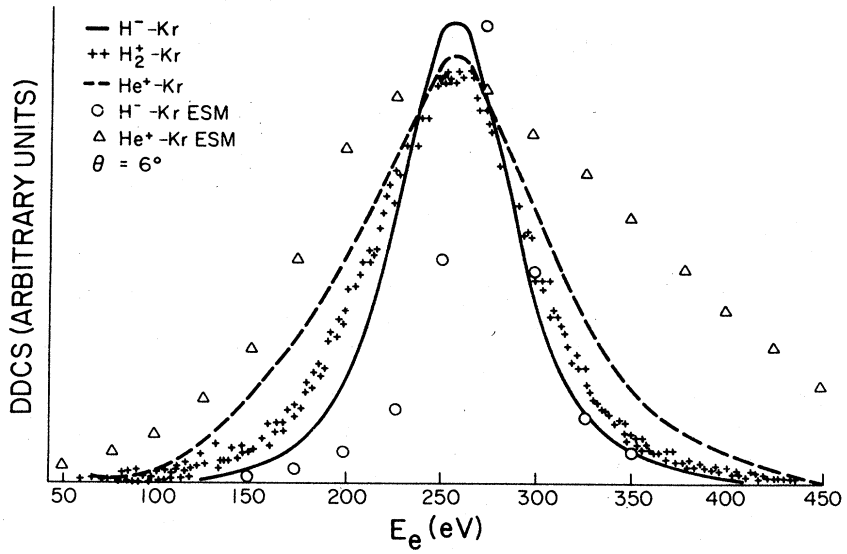

FIG. 1. Electron-loss peaks at 6° for He^+, H_2^+, and H^- collisions with Kr at an energy of 0.5 MeV/amu. Smooth curves have been drawn through the He^+ and H^- data. ESM calculations are shown for He^+ and H^- as discussed in the text.

 © 1981 The American Physical Society

model[3] of electron loss which has since been obtained from a more fundamental starting point.[4] This electron-scattering model treats the projectile electron as being free but having a velocity $\vec{v}' = \vec{v}_i + \vec{v}$, where the probability for a particular $\vec{v}$ is determined by the wave function of the bound initial state of the electron. The electron is then elastically scattered by the target from the direction given by $\vec{v}'$ to a fixed laboratory direction and detected at that laboratory angle. The probability of elastic scattering through the appropriate angle is determined by an elastic-scattering cross section. (When the acronym ESM is used here it is understood that this refers to the electron-scattering model using realistic cross sections[2] rather than a screened Coulomb potential.) Second, when the ESM double differential cross sections (DDCS) were compared to the experimental data agreement was poor. Specifically, the observed angular dependence of the electron energy at which the electron-loss peak had its maximum was not reproduced by the calculations. The experimental peak energy in the forward direction increased with increasing angle for H^- and decreased with increasing angle for H, while the ESM calculated peak energy showed no angular dependence. Furthermore, the calculated widths of the electron-loss peaks, full width at half maximum (FWHM), did not agree either in magnitude or in angular dependence with the experimental results. The ESM widths were greater than experiment when the projectile was H and were smaller when the projectile was H^-. In both cases the calculated widths were essentially independent of angle while the experimental ones tended to increase with angle in the range 0°–30°. However, the more strongly bound projectile H produced larger FWHM than H^- at the same angle, in agreement with a general prediction of the ESM.

In an attempt to further elucidate which features of electron loss have characteristics which are target and/or projectile dependent the experiments reported here were initiated. Ar, Ne, and Kr were used as target gases while H^-, He^+, and the molecular ion H_2^+ were used as projectiles. Previous experiments with He^+ and H_2^+ had shown a prominent electron-loss peak and indicated that contributions of electrons from charge transfer to the continuum to the electron-loss peak was small.[5,6] Thus we make no corrections for charge transfer. Of the three targets, Kr is the best candidate for a comparison of the electron-loss angular distribution, SDCS, with that from the elastic scattering of electrons by Kr. The electron elastic scattering angular distributions for targets Ar and Ne are structureless, showing a decrease as θ increases to about 100° and a more or less gradual rise at larger angles.[7] Kr, on the other hand, has an electron elastic scattering angular distribution which has two minima, around 80° and 135°, for electrons of energy 272 eV corresponding to $v_e = v_i$. (v_e is the electron laboratory velocity and v_i is the ion laboratory velocity.)

The projectiles H^- and He^+ have binding energies which differ by almost two orders of magnitude and thus should provide some information on the dependence of the electron-loss process on the initial state of the electron. H_2^+, being a molecular ion, should provide a test of the sensitivity of the process to the structure of the projectile. Only relative cross sections were measured and no attempt was made to determine DDCS for angles less than 1.5°.

II. RESULTS AND DISCUSSION

Figure 1 shows a comparison of the background subtracted electron-loss peaks measured at 6° for the three projectiles and the target Kr. The peak heights have been adjusted to approximately the same value. Also shown on Fig. 1 are some points resulting from an ESM calculation using optical model elastic scattering cross sections interpolated in energy and angle from the data of Ref. 7. These calculations were done only for H^- and He^+.

Figure 2 gives information concerning the angular dependences of some features of the DDCS

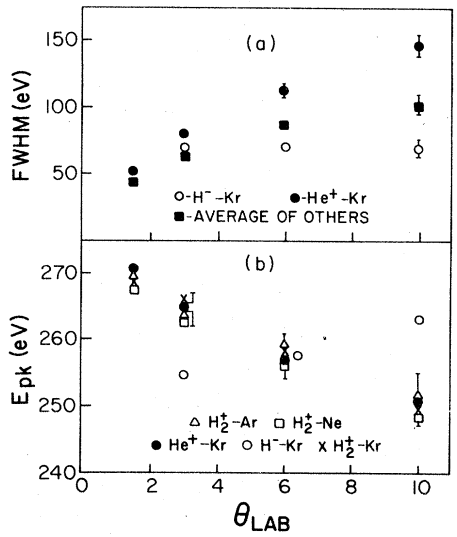

FIG. 2. Angular dependences of data. (a) Full width at half maximum of the energy-loss peak. ■ is the average of $H_2^+ - Ne$, $H_2^+ - Ar$, and $H_2^+ - Kr$, as the data was the same within experimental errors for all three targets. (b) The energy at which the peak has its maximum. Estimated errors are shown for $He^+ - Kr$. The other errors are comparable to these.

for all five collisions. E_{PK} is the energy at which the electron loss DDCS has a maximum. The error bars are our estimate of the accuracy with which the energy of the peak was determined. Also shown on Fig. 2 are the experimental values of the widths of the DDCS at half-maximum. Again the error bars are our estimate of the accuracy of the determinations.

Figure 3 shows a comparison of the angular distributions of the electron-loss electrons from the three projectiles, using Kr as a target. Also shown using the symbol X are six points obtained by an ESM calculation. These points were normalized to the H^--Kr data at $\theta = 110°$. These

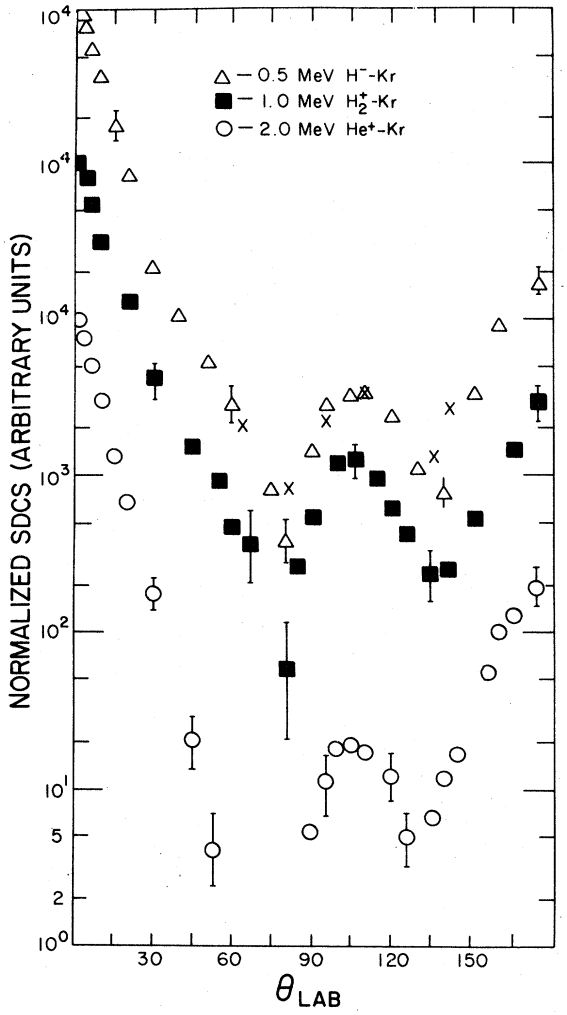

FIG. 3. The angular distributions of the electron-loss electrons in collisions with Kr at 0.5 MeV/amu. X-ESM calculations for H^- — Kr normalized to the data at $\theta = 110°$ as discussed in the text. Each of the SDCS has been normalized to 10^4 at $\theta = 1.5°$ and they have been shifted one order of magnitude relative to each other for clarity.

calculations were done in advance of the experiments in order to assure ourselves that when one integrates over velocity and angle in the ESM calculations the structure seen in e^--Kr scattering would survive. Except near the minima the error in the points is no more than ±25%. Larger error bars are shown where the data is less certain.

The DDCS shown in Fig. 1 are, at 6°, all relatively symmetric and the energy of the maxima is approximately the same for all three spectra. The widths of the spectra increase as the binding energy of the projectile increases. An ESM would predict a trend of this type. In fact, it predicts a much greater increase in width with increased binding as can be seen from the ESM calculations shown in Fig. 1. A 1s wave function was used for He^+ and the symmetrized 1s, 1s' used previously[1] was used for H^-. Clearly, the ESM does not give results which compare well with experiments using a fixed target. The symmetry evidenced by the DDCS is not maintained at all angles since, in agreement with all previous experiments, as the detection angle gets larger the DDCS lose any symmetry that they have at small angles. Of course, very near 0° the H^--Kr DDCS show a shoulder similar to those seen previously from H^--Ar and H^--He experiments.

Figure 2 shows the energy dependences of various features of the experiments. The width of the H^--Kr DDCS remains essentially constant out to an angle of 10° in agreement with earlier H^- experiments. No data is shown for H^--Kr at an angle of 1.5° because of the structure in the DDCS near 0°. The DDCS from He^+ and H_2^+ increase in width as the angle increases with, as noted before, He^+ producing wider electron loss peaks than H_2^+. The facts that the width was the same using Ar, Ne, and Kr as targets for H_2^+ as well as the similarity in the manner in which the width increases for both He^+ and H_2^+ would indicate that this increase in width is a general feature of the electron-loss process when there is a fast charged particle in the final state. Likewise, the other part of Fig. 2 shows the energy of the maxima of the electron-loss group as a function of angle. Here all data having fast charged particles in the final state have peak energies which are the same within the uncertainties in the data. Therefore we conclude that this is probably a general feature of electron loss with a bare Coulomb interaction in the final state. The H^--Kr data has a peak energy which increases with increasing angle as has been seen previously.

Figure 3 shows the angular distributions of the projectile electrons from all three projectiles using the target Krypton. It is manifestly evident

that, in the main, the structure seen in electron-scattering experiments is present. And, although only a few ESM points were calculated, it seems very likely that this model would predict a shape of the SDCS in qualitative agreement with these experimental results.

Thus, we have found some features of the experimental data which seem to be characteristic of the electron-loss process in general and some which depend specifically on the target and/or projectile. And, in view of the similarity of the experimental SDCS to electron elastic scattering, it seems clear that a detailed calculation of projectile electron loss must take into account details of target structure.

Recently, a new calculation of projectile ionization for the H-Ne and H-Ar systems has been presented.[8] For the H-Ar system these calculations are in much better agreement with experimental DDCS than any other previous calculation. The SDCS are similar to electron elastic scattering and the peak energies are dependent on the detection angle. These trends are in agreement with the experimental results we present here. However, this calculation does not include any system for which we are presenting results and thus a detailed comparison between theory and these experiments is not possible at this time.

[1]M. M. Duncan and M. G. Menendez, Phys. Rev. A 16, 1799 (1977); M. G. Menendez and M. M. Duncan, Phys. Rev. Lett. 40, 1642 (1978); Phys. Rev. A 20, 2327 (1979).
[2]M. M. Duncan and M. G. Menendez, Phys. Rev. A 19, 49 (1979).
[3]D. Burch, H. Wieman, and W. B. Ingalls, Phys. Rev. Lett. 30, 1823 (1973).
[4]F. Drepper and J. S. Briggs, J. Phys. B 9, 2063 (1976).
[5]M. G. Menendez, M. M. Duncan, F. L. Eisele, and B. R. Junker, Phys. Rev. A 15, 80 (1977); L. H. Toburen and W. E. Wilson, Phys. Rev. A 19, 2214 (1979).
[6]W. E. Wilson and L. H. Toburen, Phys. Rev. A 7, 1535 (1973); M. M. Duncan and M. G. Menendez, Phys. Lett. 56A, 177 (1976).
[7]I. E. McCarthy, C. J. Noble, B. A. Phillips, and A. D. Turnbull, Phys. Rev. A 15, 2173 (1977).
[8]D. H. Jakubassa, J. Phys. B 13, 2099 (1980).